

## Photoinduced Charge-Transfer Dehydrogenation in a Gas-Phase Metal-DNA Base Complex: Al-cytosine

David B. Pedersen,\* Marek Z. Zgierski, Stephane Denomme, and Benoit Simard

Contribution from the Steacie Institute for Molecular Sciences, National Research Council of Canada, Ottawa, Ontario, K1A 0R6, Canada

Received September 27, 2001

**Abstract:** An Al-cytosine association complex has been generated via laser ablation of a mixture of aluminum and cytosine powders that were pressed into a rod form. The ionization energy of the complex is found to be  $5.16 \pm 0.01$  eV. The photoionization efficiency spectrum of Al-cytosine has also been collected. DFT calculations indicate that binding of Al to cytosine manifests a significant weakening of the N–H bond, predicted to have a strength of 1.5 eV in the complex, and a significant stabilization of the oxo tautomeric form relative to the hydroxy forms. The predicted ionization energy of 5.2 eV agrees well with the experimental value. The threshold for dehydrogenation/ionization of Al-cytosine, forming (Al-cytosine-H)<sup>+</sup>, is found to occur at photoexcitation energies between 11.4 and 12.8 eV. This is a two-photon process that is proposed to occur via photoinduced electron transfer from Al to an antibonding ( $\sigma^*$ ) orbital localized on N–H. In the context of this mechanism, this work constitutes the first time charge transfer between a metal and DNA base has been photoinitiated in the gas phase.

### 1. Introduction

Metal centers complexed with DNA function as electron acceptors and donors and have been successfully used to study charge transport through strands of DNA.<sup>1–8</sup> Interest in such research stems from the idea that DNA is conducting and can be used as a molecular wire in molecular scale electronic devices.<sup>9,10</sup> In addition to serving as electron sources and sinks, metal centers bound to DNA have the potential to manifest novel photochemistry as well as novel dissociative pathways that can compete with the desired charge-transfer process. The effect of dissociation on the efficiency of charge transport through DNA is particularly relevant in light of theories regarding the mechanism of charge transport.<sup>10–12</sup> These theories suggest that charge transport can occur via superexchange as well as hopping mechanisms. In the latter mechanism, in the case of electron transfer, charge migration occurs via hopping of the electron

between cytosine and/or thymine bases down the length of the DNA strand. Implicit in this model is the idea that the electron can be found localized on cytosine or thymine bases for periods of time during its travel through the DNA. The attachment of relatively low energy electrons to gas-phase cytosine, however, has been shown to result in dissociation of the cytosine.<sup>13–15</sup> If analogous bond dissociation occurred in solution-phase DNA, such bond cleavage processes can be expected to dissipate a significant amount of the energy required to transport an electron and would likely result in quenching of the transfer process and a corresponding decrease in the quantum yield of electron transport. Identification of reaction pathways competing with electron transfer is therefore imperative if an understanding and subsequent optimization of electron transport in such systems is to be realized. It is also important to determine the rate of such dissociation processes. If the rate of dissociation is orders of magnitude slower than the rate of electron transfer, then dissociation will not compete effectively with the electron-transfer process. Charge (hole) transfer through synthetic oligonucleotides has been shown to occur over a range of time scales extending from picoseconds to microseconds.<sup>7,16</sup>

Consistent with a rudimentary approach to forming an understanding of the chemical properties of DNA, gas-phase studies of the nucleic bases have been carried out. In the absence of solvent, molecular dissociation can be easily identified. Furthermore, gas-phase studies are typically more amenable to theoretical interpretation, and *ab initio* studies of nucleic bases

\* To whom correspondence should be addressed. E-mail: david.pedersen@nrc.ca.

- (1) Murphy, C. J.; Arkin, M. R.; Jenkins, Y.; Ghattia, N. D.; Bossmann, S. H.; Turro, N. J.; Barton, J. K. *Science* **1993**, *262*, 1025.
- (2) Murphy, C. J.; Arkin, M. R.; Jenkins, Y.; Ghattia, N. D.; Bossmann, S. H.; Turro, N. J.; Barton, J. K. *Proc. Natl. Acad. Sci. U.S.A.* **1994**, *91*, 5315.
- (3) Arkin, M. R.; Stemp, E. D. A.; Holmlin, R. E.; Barton, J. K.; Hormann, A.; Olson, E. J. C.; Barbara, P. F. *Science* **1996**, *273*, 475.
- (4) Hall, D. B.; Holmlin, R. E.; Barton, J. K. *Nature* **1996**, *382*, 731.
- (5) Kelley, S. O.; Holmlin, R. E.; Stemp, E. D. A.; Barton, J. K. *J. Am. Chem. Soc.* **1997**, *119*, 77063.
- (6) Turro, N. J.; Barton, J. K. *JBIC, J. Biol. Inorg. Chem.* **1998**, *3*, 201.
- (7) Stemp, E. D. A.; Holmlin, R. E.; Barton, J. K. *Inorg. Chim. Acta* **2000**, *297*, 88.
- (8) Nunez, M. E.; Barton, J. K. *Curr. Opin. Chem. Biol.* **2000**, *4*, 199.
- (9) Eley, D. D.; Spivey, D. I. *Trans. Faraday Soc.* **1962**, *58*, 411.
- (10) Berlin, Y. A.; Burin, A. L.; Ratner, M. A. *Superlattices Microstruct.* **2000**, *28*, 241.
- (11) Jortner, J.; Bixon, M.; Langenbacher, T.; Michel-Beyerle, M. E. *Proc. Natl. Acad. Sci. U.S.A.* **1998**, *95*, 12759.
- (12) Giese, B.; Wessely, S.; Spormann, M.; Lindemann, U.; Meggars, E.; Michel-Beyerle, M. E. *Angew. Chem., Int. Ed.* **1999**, *38*, 996.

- (13) Chen, E. S. D.; Chen, E. C. M.; Sane, N. *Biochem. Biophys. Res. Commun.* **1998**, *246*, 228.
- (14) Chen, E. C. M.; Chen, E. S. *J. Phys. Chem. B* **2000**, *104*, 7835.
- (15) Huels, M. A.; Hahndorf, I.; Illenberger, E.; Sanche, L. *J. Chem. Phys.* **1998**, *108*, 1309.
- (16) Lewis, F. D.; Wu, T.; Liu, X.; Letsinger, R. L.; Greenfield, S. R.; Miller, S. E.; Wasielewski, M. *J. Am. Chem. Soc.* **2000**, *122*, 2889.

and base pairs have been published.<sup>17–25</sup> Benchmarks for these theoretical studies include photoionization spectra of jet-cooled guanine, uracil, and thymine, all of which have been reported.<sup>26,27</sup> The ionization energies of uracil, thymine, cytosine, and adenine have also been reported,<sup>28</sup> as has the effect of hydration on the ionization energies of adenine and thymine.<sup>29</sup> The greatest number of gas-phase studies of nucleic bases, however, has involved electron attachment and detachment processes.<sup>13–15,30–33</sup> Through these studies, the electron affinities of most nucleic bases have been established. Cytosine, for example, has a vertical electron affinity of  $-0.54$  eV, indicative of an endothermic process.<sup>30</sup> However, the adiabatic electron affinity is  $(0.56 \pm 0.05)$  eV, indicative of an exothermic process.<sup>14</sup> Both values refer to valence-bound anions, not the dipole-bound anion electron affinities.<sup>33</sup> The difference in adiabatic and vertical electron affinities is attributable to differences in the geometries of the neutral and anionic species.<sup>14</sup> In the ground state, the anion geometry is nonplanar with the  $\text{NH}_2$  and  $\text{NH}$  groups distorted out of the plane of the ring, whereas the neutral molecule possesses a plane of symmetry. Attachment of an electron to cytosine therefore generates an anion in an unstable geometry. This instability is reflected by the subsequent autodetachment of the electron or bond cleavage and dissociation of the anion that has been observed.<sup>13–15</sup>  $\text{NH}_2$ ,  $\text{H}$ , and  $\text{H}^-$  are among the fragments observed, and the internal energy required for cleavage of these fragments from the parent anion has been discussed in detail.<sup>14</sup>

The interaction of metal centers with nucleic bases is of relevance to charge-transfer processes through DNA as well as to biochemical processes. For the former, the molecular orbital structure of the metal-base complex is expected to directly affect the efficiency of charge transport through metal-DNA systems.<sup>11</sup> For the latter, there is evidence to suggest that DNA-bound metal centers can facilitate the formation of DNA base mispairs.<sup>34</sup> The effect is attributable to the stabilization of relatively unstable tautomers of the bases via interactions with the metal. Other studies of the interaction of metals with nucleic bases include gas-phase studies of  $\text{Li}^+$ ,  $\text{Na}^+$ , and  $\text{K}^+$  atomic ions with thymine and adenine.<sup>35</sup> The bond strengths of these complexes have been determined and are appropriate for metal-base bonding involving a pure ion–dipole interaction. Theoretical studies of metal ion-

nucleic base complexes have also been published.<sup>36–38</sup> In solution, metal centers have been shown to intercalate between the strands of DNA or to bind terminally to DNA.<sup>7</sup> This study also showed that DNA-bound  $\text{Os}(\text{phen})_2\text{dppz}^{2+}$  and  $\text{Ru}(\text{phen})_2\text{dppz}^{2+}$  yield similar charge-transfer rates and efficiencies, suggesting that in such ligated compounds the nature of the metal has little effect on charge transport. For bare metal centers, however, other studies suggest that the metal does affect the orbital structure of DNA bases and that this effect is metal-specific. For example, theory shows that the  $d_2$  orbital of  $\text{Pt}^{2+}$  interacts with the  $\pi$  orbitals of cytosine, while for  $\text{Hg}^{2+}$  similar interactions are relatively weak.<sup>34</sup> Gas-phase studies of the spectroscopy of metal-nucleic base systems can be expected to yield definitive information about the electronic structure of DNA bases and the effect of metals on this structure. However, to our knowledge, no gas-phase study of the spectroscopy of any metal-nucleic base complex has been conducted.

In this paper, our study of the gas-phase photochemistry and spectroscopy of an Al-cytosine complex is presented. We have found that  $\text{Al}_n\text{-cytosine}_m$  complexes can be generated via laser ablation of a pressed powder rod. This technique circumvents problems of cytosine decomposition observed in previous studies.<sup>29</sup> Typically, heating to relatively high temperatures is prerequisite to the study of cytosine in the gas phase because of the low vapor pressure of this molecule. Using a flow-tube reactor, a lower limit of  $0.4$  eV has been placed on the Al-cytosine bond energy. Also, the photochemistry and spectroscopy of the Al-cytosine complex have been examined in the  $157\text{--}308$  nm range. An ionization energy of  $5.16 \pm 0.01$  eV has been established for the molecule. The ionization efficiency spectrum of the molecule, in the  $5.21\text{--}5.69$  eV ( $238\text{--}218$  nm) range, has also been collected. Photoexcitation of the complex at  $308$  nm ( $4.03$  eV) results in dissociative loss of Al atom fragments. At energies above  $12.8$  eV, dehydrogenation of Al-cytosine is observed. DFT studies indicate that with addition of Al, the N–H bond strength decreases from  $4.1$  to  $1.5$  eV, suggesting that dehydrogenation of the Al-cyt complex occurs readily. In accord with the energetics predicted by the DFT, the mechanism of the observed dehydrogenation is proposed to be a two-photon process involving photoinduced charge transfer from Al to cytosine and subsequent decomposition resulting in dissociative loss of H or  $\text{H}^-$ . We are able to establish an upper limit of nanoseconds on the time between photoexcitation and dehydrogenation of Al-cytosine. Charge-transfer processes occurring on this time scale are therefore subject to competition from the dehydrogenation reaction.

## 2. Experimental Section

The laser ablation/photoionization mass detection apparatus has been described previously.<sup>39</sup> The only significant difference in the present experiments was the use of a pressed powder Al-cytosine rod. Al (Fisher Scientific, 20 mesh and finer) and cytosine (Aldrich, 97% pure) powders were mixed together, in an approximately 30:70% volume ratio, using a mortar and pestle. This mixture was then placed into a 6 mm diameter cylinder into which a 6 mm piston was forced by applying a pressure of  $2500$  psi ( $1.7 \times 10^7$  Pa). Pressure was maintained for approximately

- (17) Callis, P. R. *Annu. Rev. Phys. Chem.* **1983**, *34*, 329.
- (18) Petke, J. D.; Maggiora, G. M.; Christoffersen, R. E. *J. Phys. Chem.* **1992**, *96*, 6992.
- (19) Fulscher, M. P.; Roos, B. O. *J. Am. Chem. Soc.* **1995**, *117*, 2089.
- (20) Colominas, C.; Luque, F. J.; Orozco, M. *J. Am. Chem. Soc.* **1996**, *118*, 6811.
- (21) Hobza, P.; Sponer, J. *Chem. Rev.* **1999**, *99*, 3247.
- (22) Shukla, M. K.; Mishra, P. C. *Chem. Phys.* **1999**, *240*, 319.
- (23) Aleman, C. *Chem. Phys.* **2000**, *253*, 13.
- (24) Barsky, D.; Colvin, M. E. *J. Phys. Chem. A* **2000**, *104*, 8570.
- (25) Desfrancois, C.; Carles, S.; Schermann, J. P. *Chem. Rev.* **2000**, *100*, 3943.
- (26) Nir, E.; Grace, L.; Brauer, B.; de Vries, M. S. *J. Am. Chem. Soc.* **1999**, *121*, 4896.
- (27) Brady, B. B.; Peteanu, L. A.; Levy, D. H. *Chem. Phys. Lett.* **1988**, *147*, 538.
- (28) Hush, N. S.; Cheung, A. S. *Chem. Phys. Lett.* **1975**, *34*, 11.
- (29) Kim, S. K.; Wellington, L.; Herschbach, D. R. *J. Phys. Chem.* **1996**, *100*, 7933.
- (30) Aflatooni, K.; Gallup, G. A.; Burrow, P. D. *J. Phys. Chem. A* **1998**, *102*, 6205.
- (31) Desfrancois, C.; Periquet, V.; Bouteiller, Y.; Schermann, J. P. *J. Phys. Chem. A* **1998**, *102*, 1274.
- (32) Hendricks, J. H.; Lyapustina, S. A.; de Clercq, H. L.; Bowen, K. H. *J. Chem. Phys.* **1998**, *108*, 8.
- (33) Schiedt, J.; Weinkauff, R.; Neumark, D. M.; Schlag, E. W. *Chem. Phys.* **1998**, *239*, 511.
- (34) Sponer, J.; Sponer, J. E.; Gorb, L.; Leszczynski, J.; Lippert, B. *J. Phys. Chem. A* **1999**, *103*, 11406.
- (35) Rodgers, M. T.; Armentrout, P. B. *J. Am. Chem. Soc.* **2000**, *122*, 8548.

- (36) Burda, J. V.; Sponer, J.; Hobza, P. *J. Phys. Chem.* **1996**, *100*, 7250.
- (37) Burda, J. V.; Sponer, J.; Leszczynski, J.; Hobza, P. *J. Phys. Chem. B* **1997**, *101*, 9670.
- (38) Sponer, J.; Burda, J. V.; Sabat, M.; Leszczynski, J.; Hobza, P. *J. Phys. Chem. A* **1998**, *102*, 5951.
- (39) Jakubek, Z. J.; Simard, B. *J. Chem. Phys.* **2000**, *112*, 1733.

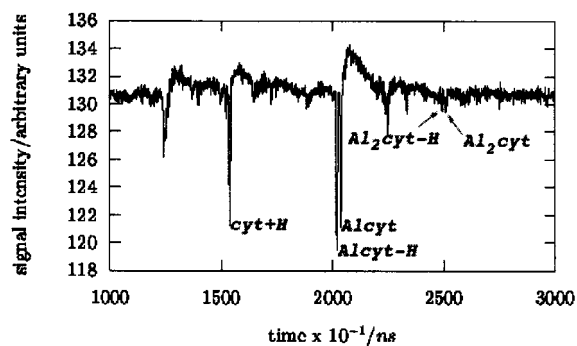


**Figure 1.** The mass spectrum collected when 157 nm laser light was used to ionize species generated via laser ablation of an Al-cytosine pressed powder rod. Species containing both Al and cytosine are observed, some of which are labeled. cyt denotes cytosine.

5 min after which the pressed rod was removed and placed in the ablation chamber of the apparatus. Ablation of the rod with approximately  $500 \mu\text{J pulse}^{-1}$  355 nm laser (Lumonics YM200) light, focused to an  $\sim 1 \text{ mm}^2$  spot, synchronous with a He pulse of 2.1  $\mu\text{s}$  duration (piezoelectric valve with  $\sim 80 \text{ psi}$  ( $6 \times 10^5 \text{ Pa}$ ) backing pressure) passed over the rod, generated  $\text{Al}_n\text{cyt}_m$  species, where cyt denotes cytosine, entrained in He. Source conditions were adjusted to maximize the Al-cyt signal intensity. These species then underwent expansion into the  $10^{-6}$  Torr ( $10^{-4} \text{ Pa}$ ) vacuum of the first chamber. In the second chamber, species were ionized using laser light of varying wavelength. Ionization laser fluences were measured using OPHIR/NOVA and Gentec Duo/ED-500 power meters.

The flow-tube apparatus has also been described previously.<sup>40–42</sup> In these experiments, the pressed Al-cytosine rod was ablated with  $\sim 80 \text{ mJ pulse}^{-1}$  308 nm laser light focused to a 1 mm diameter spot. A continuous flow of He (15 000 sccm) was maintained over the rod. The laser-generated plasma was entrained in the He flow and forced through a 1 cm long 2 mm diameter channel before expanding into the 1.0 Torr (130 Pa) pressure maintained in the flow tube. The temperature of the tube was varied from 260 to 340 K for different runs. Species were ionized with the unfocused  $40 \text{ mJ pulse}^{-1}$  193 nm output of a Lumonics EX700 laser and detected using the reflectron time-of-flight mass spectrometer.

### 3. Results

With laser ablation of the Al-cytosine rod and subsequent ionization with the 157 nm output of an  $\text{F}_2$  laser, the mass spectrum shown in Figure 1 was collected. Peaks with flight times appropriate for species cyt + H, Alcyt-H, Alcyt,  $\text{Al}_2\text{cyt-H}$ , and  $\text{Al}_2\text{cyt}$  are labeled. Interestingly, with 157 nm ionization, dehydrogenation of  $\text{Al}_n\text{cytosine}_m$  species was observed, while for metal-free molecules only species of the form  $\text{cyt}_n\text{H}_m$  were observed. Both post-excitation and plasma-induced events (i.e., reactions, dissociations, etc.) in the detection and source regions of the experiment, respectively, can affect the distribution of species observed in the mass spectrum. To investigate the post-excitation chemistry of Al-cytosine, the ionization wavelength was varied. In Figure 2, the relative amount of dehydrogenated species is observed to decrease as the ionization laser wavelength is increased. The dependence of the Alcyt-H:Alcyt peak intensity ratio on the ionization laser wavelength suggests that photoexcitation is the process responsible for dehydrogenation. Similarly, an increase in the relative intensity of  $\text{Al}_2\text{cyt}$  as the

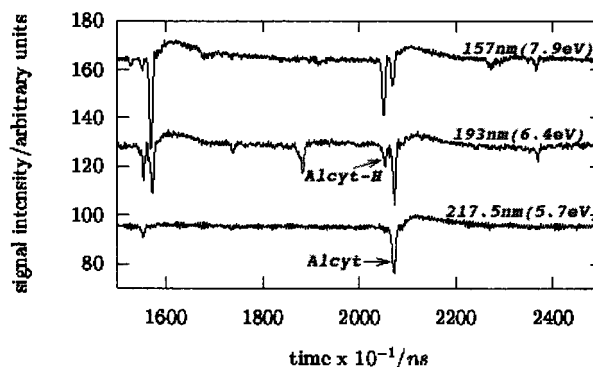


**Figure 2.** The Al-cytosine region of the mass spectra collected upon ionization with 157, 193, and 217.5 nm laser light. Alcyt denotes Al-cytosine, and Alcyt-H denotes dehydrogenated Al-cytosine. Alcyt-H is observed at 157 and 193 nm but not at 217.5 nm.

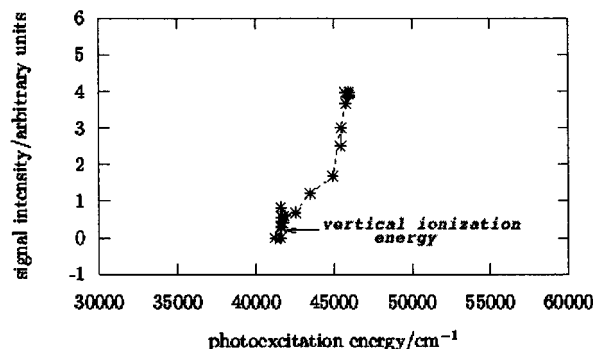


**Figure 3.** The photoionization efficiency spectrum of Al-cytosine. The signal intensity has been corrected for changes in laser power. The data collected are shown as points, and the line joining them is a guide to the eye. The onset of signal is marked as the vertical ionization energy.

ionization wavelength was increased (data not shown) is indicative of loss of  $\text{Al}_2\text{cyt}$  at lower wavelengths possibly as a result of post-excitation dissociation of the complex. No correlation between loss of  $\text{Al}_2\text{cyt}$  and growth of Alcyt-H, as the ionization wavelength was varied, was observed.

Evidence of dissociation was also observed to occur at longer wavelengths. Excitation of Alcyt with high intensity ( $50 \text{ mJ cm}^{-2} \text{ pulse}^{-1}$ ) 308 nm radiation 15 ns before excitation with 157 nm light resulted in major depletion of Alcyt and Alcyt-H. Concurrent, large growth in the intensity of the Al atom mass spectral peak was observed. These observations indicate that pre-excitation with 308 nm results in Al atom formation as a result of dissociation of the  $\text{Al}_n\text{cyt}$  and/or  $\text{Al}_n\text{cyt-H}$  species. The contribution of two-photon processes to Alcyt-H:Alcyt intensity ratio was investigated by varying the intensity of the excitation laser. These data are presented below.

In Figure 3, the photoionization efficiency spectrum of Alcyt, in the 5.21–5.69 eV (238–218 nm) range, is shown. The spectrum has been corrected for variance in laser power over this range. The ionization energy of Alcyt is marked on the figure. At energies well above the ionization energy, the signal intensity is observed to increase significantly.

In Figure 4, a sample mass spectrum collected using the flow-tube apparatus is shown. The spectrum was collected at 273 K at a flow-tube pressure of 1.0 Torr (130 Pa). In addition to having different source conditions (see above), the Al-cytosine pressed powder rod used in the flow-tube experiments had a higher Al content than the rod used in the photoionization

(40) Pedersen, D. B.; Parnis, J. M.; Rayner, D. M. *J. Chem. Phys.* **1998**, *109*, 551.

(41) Mitchell, S. A.; Lian, L.; Rayner, D. M.; Hackett, P. A. *J. Chem. Phys.* **1995**, *103*, 5339.

(42) Lian, L.; Mitchell, S. A.; Rayner, D. M. *J. Chem. Phys.* **1994**, *98*, 11637.



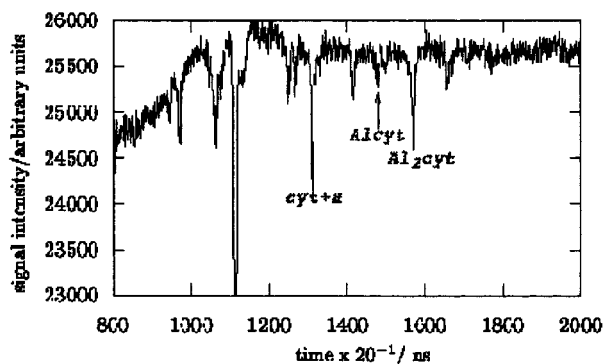


**Figure 4.** The mass spectrum acquired using the flow-tube apparatus. The flow-tube temperature was 273 K, and the bath gas pressure was 1.0 Torr (130 Pa). Peaks corresponding to Al-cytosine (Alcyt) and Al<sub>2</sub>-cytosine (Al<sub>2</sub>cyt) are labeled. In the configuration employed, the mass resolution of the instrument was insufficient to resolve dehydrogenated Al-cytosine or Al<sub>2</sub>-cytosine from nondehydrogenated species.

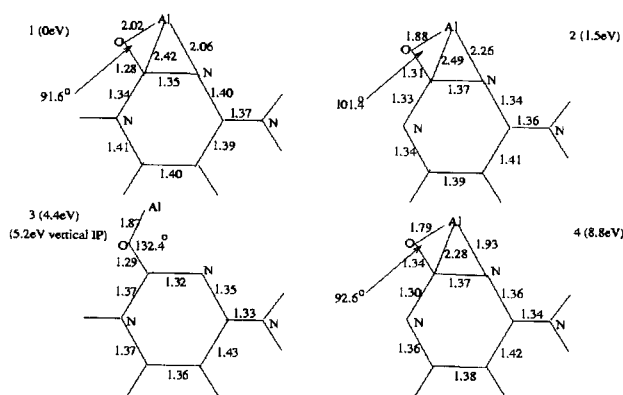


**Figure 5.** Lowest energy structures of Al-cytosine (1), dehydrogenated Al-cytosine (2), Al-cytosine cation (3), and dehydrogenated Al-cytosine cation (4). Bond lengths are given in Ångströms. Energies of formation, relative to neutral Al-cytosine, are given in eV units.

experiments. Accordingly, the Al<sub>2</sub>cyt signal is larger than the Alcyt signal in Figure 4 but not in Figure 1. The resolution in Figure 4 is less than that of Figure 1, so dehydrogenated species cannot be distinguished from the parent molecules. Alcyt signals of intensity comparable to that seen in Figure 4 were observed in the flow-tube experiments at 263, 273, and 343 K.

## 4. Discussion

**4.1. Al-cytosine Interactions.** The excitation–dissociation–ionization photochemistry and spectroscopy observed involve neutral, ionic, dissociated neutral, and dissociated ionic species. To facilitate interpretation of the experimental findings, the geometries and relative energies of the ground states of these species were determined using DFT. The B3LYP functionals and 6-31G\* basis set were employed. An overview of the results is shown in Figure 5. As a calibration, it is noteworthy that the 5.2 eV vertical ionization energy predicted by DFT compares favorably with the experimentally determined  $5.16 \pm 0.01$  eV value. The theory also predicts significantly different geometries for the neutral and cationic Al-cyt species. Accordingly, the Franck–Condon factors associated with transitions near the ionization threshold are expected to be relatively small. This prediction is consistent with the relatively low signal intensity observed in Figure 3 near the ionization threshold.

On the basis of the geometry shown in Figure 5, Al is predicted to form an association complex with cytosine. This

prediction is consistent with the observation of Al fragments upon 308 nm dissociation of Al-cyt. For an insertion complex, dissociation of the molecule can be expected to yield Al-containing fragments such as AlH, AlC, or AlN. On the contrary, polyatomic Al-containing fragments are not observed in any of the mass spectra collected. Thus, an insertion geometry seems unlikely. Accordingly, Al-cytosine is likely an association complex. Al is also known to form association complexes with benzene and toluene.<sup>43</sup>

For an association complex, bonding interactions are expected to be relatively modest. However, according to DFT, the Al does coordinate with three different atoms (N, C, and O), and the overall bonding interaction may be relatively strong. To ascertain the bond strength, flow-tube experiments were conducted. The flow-tube results provide a lower limit of the strength of the bond formed between Al and cytosine. The higher temperatures achievable in the flow-tube apparatus can be used to distinguish van der Waals complexes, possibly formed in the extremely cold environment associated with jet expansion in the photoionization apparatus, from covalently or datively bound complexes. A binding energy of at least 0.4 eV is necessary for a species to be observed in the flow-tube apparatus at room temperature. Typically, at lower binding energies, dissociation of the association complex will be efficient, and the signal intensity of the complex will be too weak to be observed. The observation of Al-cyt in the flow-tube mass spectra, shown in Figure 4, therefore allows a lower limit of 0.4 eV to be placed on the Al-cyt binding energy. A binding energy of this magnitude is also consistent with the fact that the Alcyt signal intensity, in the flow-tube experiments, did not change significantly over the 263–343 K range. The DFT predicts an Al-cytosine binding energy of 1.7 eV, consistent with the 0.4 eV lower limit value.

Overall, the DFT seems to yield accurate energetics and geometries for the Al-cytosine species of interest. Accordingly, some conclusions regarding the effect of Al on the properties of cytosine can be drawn from the DFT results. Perhaps the most interesting is the predicted decrease in N–H bond strength that accompanies addition of Al to cytosine. The energy difference between Al-cyt and the dehydrogenated species, shown in Figure 5, is 1.5 eV. By comparison, the predicted N–H bond strength in cytosine is 4.1 eV.<sup>13</sup> The presence of Al therefore manifests a 2.6 eV stabilization of the dehydrogenated species. The stabilization appears to occur via donation of charge from the Al to the cytosine ring. This ring is remarkably aromatic, with all ring-constituent bond lengths falling in the  $1.37 \pm 0.03$  Å range in both hydrogenated and dehydrogenated Al-cyt. The three Al bonds lengths, however, change significantly upon dehydrogenation as seen in Figure 5. There is also a slight increase in the charge on Al, as determined by a Mulliken population analysis, going from +0.27 to +0.34 upon dehydrogenation. Both of these factors suggest that charge donation from Al to cytosine is responsible for the stabilization of the dehydrogenated Al-cyt and the relatively low N–H bond strength.

The presence of Al also affects the relative stabilities of the oxo and hydroxy tautomers of cytosine. For cytosine, three tautomers are predicted to be energetically equivalent, with heats

(43) Hair, G. S.; Cowley, A. H.; Jones, R. A.; McBurnett, B. G.; Voigt, A. J. *Am. Chem. Soc.* **1999**, *121*, 4922.

of formation within a few kilocalories of each other.<sup>20</sup> With the addition of Al, however, the oxo tautomer shown in Figure 5 is the most stable with the next most stable tautomer lying 0.9 eV higher in energy. Such stabilization of specific tautomers is an effect similar to that which occurs upon addition of metal cations to DNA bases.<sup>34</sup> However, to our knowledge, this is the first evidence that neutral metal atoms have a similar effect. As stabilization of specific tautomers can impact the formation of DNA base mismatches, the role of neutral metallic species in relevant biochemistry may need to be considered in more detail. With respect to our gas-phase studies, we see no evidence of tautomer-specific chemistry suggesting that only the most stable species, the oxo tautomer shown in Figure 5, is present in sufficient quantity to be observed.

Finally, the addition of Al to cytosine manifests a significant lowering of the ionization energy. Cytosine has an ionization energy of 8.94 eV,<sup>28</sup> while the vertical ionization energy of Al-cyt is  $5.16 \pm 0.01$  eV. From DFT it is seen that the charge in the cation is centered almost entirely on the Al, which a Mulliken analysis predicts to have a charge of +0.86. In a simplistic picture, the (Al-cyt)<sup>+</sup> cation can be thought of as an Al<sup>+</sup> cation. Al has an ionization energy of 5.98 eV,<sup>44</sup> bound to cytosine. Interactions with cytosine have a stabilizing effect and lower the energetic cost of removal of the electron from Al to the observed  $5.16 \pm 0.01$  eV value. The implications of these findings are that an electron can effectively be removed from the Al specifically and the Al therefore serves as a potential electron source. Photoinduced charge transfer from the Al to the cytosine should therefore be possible, and exploitation of such metal-DNA base complexes for the study of charge-transfer phenomena involving DNA bases and oligomers in the gas phase is feasible.

#### 4.2. Photoinduced Charge-Transfer Dehydrogenation.

Various possible mechanisms for the observed photoinduced dehydrogenation can be envisioned, and these are considered below. All of them involve resonance-enhanced absorption of two photons. That absorption of two photons is prerequisite for the dehydrogenation can be determined from energetic considerations. On the basis of the DFT energies shown in Figure 5, the threshold for formation of dehydrogenated Al-cyt cation, (Al-cyt-H)<sup>+</sup>, is 8.8 eV. As this energy is well above the 6.4 eV threshold photon energy at which dehydrogenation occurs (Figure 2), the (Al-cyt-H)<sup>+</sup> observed must result from a two-photon process.

To address the issue of multiphoton contributions to the dehydrogenation process, the dependence of the Al-cyt and Al-cyt-H signal intensities on ionization laser intensity can be examined. As is typical, the ion signal intensity can be assumed to have a power dependence on the laser intensity<sup>45</sup>

$$I_S = \sigma I_L^n \quad (1)$$

where  $\sigma$  is the effective absorption cross section, and  $I_S$  and  $I_L$  are the mass spectral signal intensity and ionization laser intensity, respectively. In accord with eq 1, a plot of  $\ln(I_S)$  against  $\ln(I_L)$  should give a straight line with a slope equal to  $n$ , the number of photons involved in formation of the ion. In

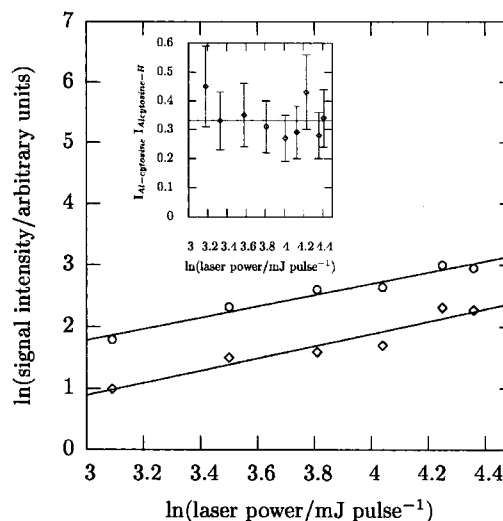


**Figure 6.** The dependence of signal intensity on ionization laser power for both Al-cytosine and dehydrogenated Al-cytosine. The slopes of both lines are one, within experimental error. Inset shows the ratio of Al-cytosine signal intensity to that of dehydrogenated Al-cytosine. No significant change in the ratio occurs over the range of laser powers shown.

Figure 6, such plots are shown for (Al-cyt)<sup>+</sup> and (Al-cyt-H)<sup>+</sup> for an excitation laser wavelength of 193 nm. The slopes of both plots are one, within experimental error. Photogeneration of these species therefore involves absorption of a single photon as the rate-limiting step. This result is consistent with the occurrence of resonant-enhanced dehydrogenation of Al-cyt, where the dissociation process occurs via population of an intermediate state of Al-cyt. Additionally, as seen in Figure 6, the intensity of the Al-cyt peak relative to the Al-cyt-H peak is invariant as laser power is varied. If dehydrogenation involves absorption of two photons simultaneously, not sequentially, then a quadratic dependence of  $I_S$  on  $I_L$  is predicted by eq 1. Ionization, however, is a single-photon process, as indicated by the good agreement between the predicted and the observed vertical ionization energies. In this case, the Al-cyt-H peak intensity will increase relative to that of Al-cyt as laser power is increased, contrary to Figure 6. The invariance of this peak intensity ratio is further indication that dehydrogenation is the result of a resonant two-photon process. In light of this evidence, the contribution of nonresonant two-photon processes to the Al-cytosine and Al-cyt-H peak intensities observed is likely insignificant.

Of the possible mechanisms of dehydrogenation, some can be precluded. All statistical dissociation (RRKM) processes involving neutral Al-cytosine can be expected to manifest cleavage of Al-(cytosine) bonds, of which there are three (Figure 5) having an average strength of 0.6 eV, as these are the weakest bonds in the molecule. Thus, mechanisms involving statistical N-H bond cleavage, specifically, of neutral Al-cyt are highly improbable. Processes involving formation of the Al-cyt cation as an intermediate are also unlikely. As seen in Figure 5, the geometry of this species is distinct from that of the neutral and of the dehydrogenated cation. Accordingly, Franck-Condon factors associated with optical transitions between the ground state of the cation and either the ground state of the neutral Al-cyt or the ground state of the ionic dehydrogenated species are expected to be small. The Al-cyt-H signal intensities observed, however, are relatively strong, inconsistent with

(44) Moore, C. E. *Atomic Energy Levels*; National Bureau of Standards, 1949; Vol. 1.

(45) Fisanick, G. L.; Eichelberger, T. S.; Heath, B. A.; Robin, M. B. *J. Chem. Phys.* **1980**, *72*, 5571.

participation of ground state  $(\text{Al-cyt})^+$  in the dehydrogenation process. Population of electronically excited states of the cation, with geometries more comparable to those of the neutral and ionic dehydrogenated species, as intermediates in the dehydrogenation process is also unlikely. According to DFT, the lowest electronically excited state of  $(\text{Al-cyt})^+$  is predicted to occur 5 eV above the ground state and cannot be populated directly from the ground state of the neutral species, using the experimental photon energies.

The first of the two most plausible mechanisms for photoinduced dehydrogenation/ionization of Al-cyt involves sequential dehydrogenation and ionization steps. Having precluded statistical dissociation, the former must occur via population of an electronic state ( $\sigma^*$ ) that is repulsive in the N–H coordinate. At threshold (less than 6.4 eV as seen in Figure 2), N–H bond cleavage is energetically possible requiring only 1.5 eV (see Figure 5). Ionization of the dehydrogenated Al-cyt fragment, however, is predicted to require 7.3 eV. For this to occur via 6.4 eV photoexcitation (i.e., absorption of a second photon), the fragment must be created with at least 0.9 eV of internal energy. Creation of the Al-cyt-H in an electronically excited state is not likely because with 6.4 eV excitation, access to only the lowest  $\sigma^*$  state of Al-cyt, correlating with ground-state fragments, is expected to be possible. Alternatively, the dehydrogenation can leave the Al-cyt-H fragment with 0.9 eV of vibrational energy. To first order, the amount of internal energy imparted to the fragment can be estimated using the impulsive model.<sup>46</sup> The model predicts that dissociation of Al-cyt on a repulsive surface imparts less than 0.5 eV to the internal energy of the Al-cyt-H fragment. This energy is less than the 0.9 eV required and insufficient for ionization to occur via absorption of a 6.4 eV photon. In light of this evidence, a sequential dehydrogenation/ionization mechanism cannot be completely precluded, but seems much less likely than a concerted mechanism.

A concerted mechanism involves resonant-enhanced absorption of two photons directly to a highly excited ( $6.4 + 6.4 = 12.8$  eV) state of neutral Al-cyt from which ionization/dehydrogenation occurs spontaneously. From the DFT calculations, in the final product  $(\text{Al-cyt-H})^+$  the charge is centered almost entirely on the Al. A Mulliken population analysis assigns a charge of +0.87 to Al. Overall, therefore, the ionization/dehydrogenation process results in removal of an electron from Al and cleavage of the N–H bond. For a concerted mechanism, this process would have to involve a charge-transfer state with positive charge on Al and negative charge localized in the neighborhood of N–H (likely in a  $\sigma^*$  type orbital). The presence of the localized negative charge manifests loss of  $\text{H}^-$  or loss of H and subsequent autoionization of Al-cyt-H. In support of this mechanism, cytosine itself has an absorption coefficient of 0.5–1.0 in the 5–7 eV range<sup>17,18</sup> and has multiple electronic states in this region so that a high density of states can be expected. The probability of facile resonant-enhanced two-photon absorption is therefore likely relatively high over the range of experimental energies where dehydrogenation is observed. Also, the probability of optical excitation to charge-transfer states is well known to be high due to very large oscillator strengths associated with such transitions.<sup>47,48</sup> There-

fore, the occurrence of resonant-enhanced two-photon excitation to the proposed charge-transfer state is very plausible. Furthermore, electron attachment to gas-phase cytosine is known to result in loss of  $\text{H}^-$ .<sup>15</sup> The concerted/charge-transfer mechanism is therefore the most plausible mechanism for the observed ionization/dehydrogenation of Al-cytosine.

The likelihood of this mechanism is further supported by considering  $\text{Al}_2$ -cytosine dehydrogenation. In the context of the mechanism proposed, photoinduced charge transfer and subsequent loss of H or  $\text{H}^-$  should occur with any complex of a metal center with cytosine provided that covalent interactions are modest so that the chemical properties of the complexed cytosine moiety do not differ very much from those of cytosine in the Al-cyt complex. In this case, photoinduced charge transfer from the metal to the orbital localized on N–H ( $\sigma^*$ ) of cytosine will manifest dehydrogenation. The energetics of the process, however, can be expected to change with the ionization energy of the metal center. For  $\text{Al}_2$ , the  $5.989 \pm 0.002$  eV ionization energy<sup>49</sup> is very similar to that of Al (5.984 eV),<sup>44</sup> and the onset of dehydrogenation of  $\text{Al}_2$ -cyt can therefore be expected to occur between 5.7 and 6.4 eV, as is the case for Al-cytosine. Indeed, the threshold for dehydrogenation of  $\text{Al}_2$ -cyt is observed to occur in this region consistent with the proposed mechanism. Dehydrogenated  $\text{Al}_2$ -cyt is observed in Figure 1, for example. The observation of such dehydrogenation lends further credence to the concerted/charge-transfer mechanism of dehydrogenation proposed.

For H or  $\text{H}^-$  loss from cytosine to compete effectively with charge-transfer processes, the rate of the two processes must be comparable. In solution, charge transport through DNA has been measured and occurs over the  $10^{-6}$ – $10^{-12}$  s time scale.<sup>7,16</sup> In our apparatus, photoexcitation occurs between the acceleration plates of the time-of-flight mass spectrometer. Ions are therefore immediately accelerated out of the source and toward the detector. Delayed ionization/dehydrogenation of Al-cytosine on the hundreds of nanoseconds time scale would manifest a significant increase in the time between photoexcitation and the time of impact of the ion with the detector. Such an increase in flight time is not observed. Instead, peaks corresponding to Al-cytosine and Al(cyt-H) appear where expected for ions of this mass produced by prompt ionization processes. Furthermore, both peaks are sharp. The absence of any significant broadening of these peaks indicates that any dissociation must be occurring on the time scale of 100 ns or less. In the gas phase, the rate of dissociative loss of H or  $\text{H}^-$  is therefore fast enough to compete with charge-transfer processes occurring on this time scale. The gas-phase rate also falls within the  $10^{-6}$ – $10^{-12}$  s time scale observed in solution-phase charge-transport processes through DNA suggesting that loss of H or  $\text{H}^-$  can compete effectively with charge transfer. The effect of solvent on the rate and energetics of the solution-phase reaction, however, remains to be determined.

## 5. Summary and Conclusions

It has been demonstrated that laser ablation of pressed-powder rods can be used to generate gas-phase, neutral metal-nucleic base complexes. This technique has been used to collect the photoionization efficiency spectrum of Al-cyt and to study

(46) Okabe, H. *Photochemistry of Small Molecules*; Wiley and Sons: New York, 1978.

(47) Mulliken, R. S. *J. Am. Chem. Soc.* **1952**, *74*, 811.

(48) Syage, J. A.; Felker, P. M.; Zewail, A. H. *J. Chem. Phys.* **1984**, *81*, 2233.

(49) Harrington, J. E.; Weisshaar, J. C. *J. Chem. Phys.* **1990**, *93*, 854.

dissociation processes of this molecule. Al-cytosine is found to form an association complex. From flow-tube experiments, a lower limit of 0.4 eV, on the Al-cyt binding energy, has been established. DFT predicts an Al-(cytosine) bond strength of 1.7 eV. The complex has a vertical ionization energy of  $5.16 \pm 0.01$  eV. Both DFT and experimental signal intensities, being relatively weak near the ionization threshold, indicate that the Franck–Condon overlap between the ground states of the neutral and ionic Al-cyt species is poor. The neutral and ionic species are predicted to have significantly different geometries, accordingly. For the neutral species, Al is found to manifest a significant weakening of the N–H bond. The bond strength is predicted to be 1.5 eV.

The most significant result of this work is the observation of photoinduced dehydrogenation of Al-cyt. The threshold for

dehydrogenation of Al-cyt has been shown to lie between 11.4 and 12.8 eV. Also, an upper limit of 100 ns has been set on the time between photoexcitation and dehydrogenation. It has been shown that photoinduced, intramolecular electron transfer from Al to an antibonding ( $\sigma^*$ ) orbital localized on N–H, and subsequent dissociation, is the most plausible mechanism of dehydrogenation. In the context of this mechanism, these results constitute the first demonstration of photoinduced electron transfer from a metal center to a DNA base in the gas phase. As Al-cyt is a prototype system for metal–DNA interactions, this technique may therefore hold promise as a means of studying electron-transfer processes through DNA *in the gas phase*.

JA0122501